


FULL PAPER

Open Access



Low-energy particle experiments–electron analyzer (LEPe) onboard the Arase spacecraft

Yoichi Kazama^{1*} , Bo-Jhou Wang¹, Shiang-Yu Wang¹, Paul T. P. Ho¹, Sunny W. Y. Tam², Tzu-Fang Chang³, Chih-Yu Chiang² and Kazushi Asamura⁴

Abstract

In this report, we describe the low-energy electron instrument LEPe (low-energy particle experiments–electron analyzer) onboard the Arase (ERG) spacecraft. The instrument measures a three-dimensional distribution function of electrons with energies of ~ 19 eV–19 keV. Electrons in this energy range dominate in the inner magnetosphere, and measurement of such electrons is important in terms of understanding the magnetospheric dynamics and wave–particle interaction. The instrument employs a toroidal tophat electrostatic energy analyzer with a passive 6-mm aluminum shield. To minimize background radiation effects, the analyzer has a background channel, which monitors counts produced by background radiation. Background counts are then subtracted from measured counts. Electronic components are radiation tolerant, and 5-mm-thick shielding of the electronics housing ensures that the total dose is less than 100 kRad for the one-year nominal mission lifetime. The first in-space measurement test was done on February 12, 2017, showing that the instrument functions well. On February 27, the first all-instrument run test was done, and the LEPe instrument measured an energy dispersion event probably related to a substorm injection occurring immediately before the instrument turn-on. These initial results indicate that the instrument works fine in space, and the measurement performance is good for science purposes.

Keywords: Low-energy electron measurement, Particle instrumentation, Inner magnetosphere

Introduction

ERG (Exploration of Energization and Radiation in Geospace) is a science project to explore the inner magnetosphere (Miyoshi et al. 2012). The objectives of the project are to understand acceleration mechanisms of electrons in the outer radiation belt, dynamics of space storms and substorms, and wave–particle interactions driving particle precipitation to the ionosphere. The project consists of the satellite observation team, the ground-based observation team, and the computer simulation team. The spacecraft observation team and Japan Aerospace Exploration Agency (JAXA) developed the Arase (ERG) satellite for in situ observations of plasma particles and

waves (Miyoshi et al. 2017). The spacecraft was successfully launched into orbit on December 20, 2016, from Kagoshima, Japan.

For the Arase spacecraft, Academia Sinica Institute of Astronomy and Astrophysics (ASIAA) and Institute of Space and Plasma Sciences (ISAPS) at National Cheng Kung University (NCKU) in Taiwan developed the electron instrument LEPe (low-energy particle experiments–electron analyzer), in collaboration with JAXA.

In the framework of the ERG project, the targets of the low-energy electron observations by the LEPe instrument are:

- To measure dominant electron environments that govern the structures of the inner magnetosphere where high-energy electrons are produced,

*Correspondence: kazama.yoichi@asiaa.sinica.edu.tw

¹ Academia Sinica Institute of Astronomy and Astrophysics, No.1, Sec. 4, Roosevelt Rd, Taipei 10617, Taiwan

Full list of author information is available at the end of the article

- To identify source electrons for plasma waves that can accelerate medium-energy electrons up to an MeV range by wave–particle interactions,
- To observe loss cone filling due to resonant interactions of plasma-sheet electrons with plasma waves in the inner magnetosphere.

The LEPe instrument was designed to measure electrons with energies from ~ 20 eV to ~ 20 keV. These electrons correspond to the main component of plasmas in the inner magnetosphere. Electrons above ~ 10 keV are covered by the MEPe (medium-energy particle experiments–electron analyzer) instrument (Kasahara et al. 2017). To identify pitch angle anisotropy, LEPe measures three-dimensional electron fluxes every spin (~ 8 s). The angular resolutions are ~ 22.5 deg in the azimuth and elevation directions, which enables to derive electron's parallel and perpendicular temperatures and pitch angle distributions. For the loss cone measurement, because a typical loss cone angle is expected to be several degrees at the equator, fine angular channels resolving in several degrees can measure electron fluxes both in and out of a loss cone for identifying strong pitch angle diffusion.

In summary, to fulfill the science targets of the low-energy electron observation, measurement requirements of the LEPe instrument are: (1) measurement energy range from a few tens eV to ~ 20 keV, (2) three-dimensional flux measurement with angular resolutions of ~ 22.5 deg, and (3) fine angular measurement with a resolution less than several degrees.

Overview

Figure 1 shows a photograph of the flight model of the LEPe instrument. The instrument is 268.5 mm tall and weighs 5.51 kg. The instrument consists of two parts: the ‘sensor’ housing and the ‘PSU’ (power supply unit) housing. The cylindrically shaped sensor housing includes an electrostatic energy analyzer and electronics. The PSU housing is a case for PSUs below the sensor housing. In the photograph, the instrument is placed upside down; therefore, the analyzer is on the bottom and the PSU housing is on the top. The specifications of the instrument are summarized in Table 1.

These two housings are attached at the mounting flange, which is used to install the instrument onto the spacecraft side panel. The sensor housing extends outside the spacecraft body to have a field of view (FOV) without interference from other components on the spacecraft panels. Since the sensor housing receives heat from sun light, chromate conversion coating is applied to the sensor housing to lower sun light absorption. The solar absorptivity α of the coating was measured with test pieces to be ~ 0.16 . Furthermore, conductive

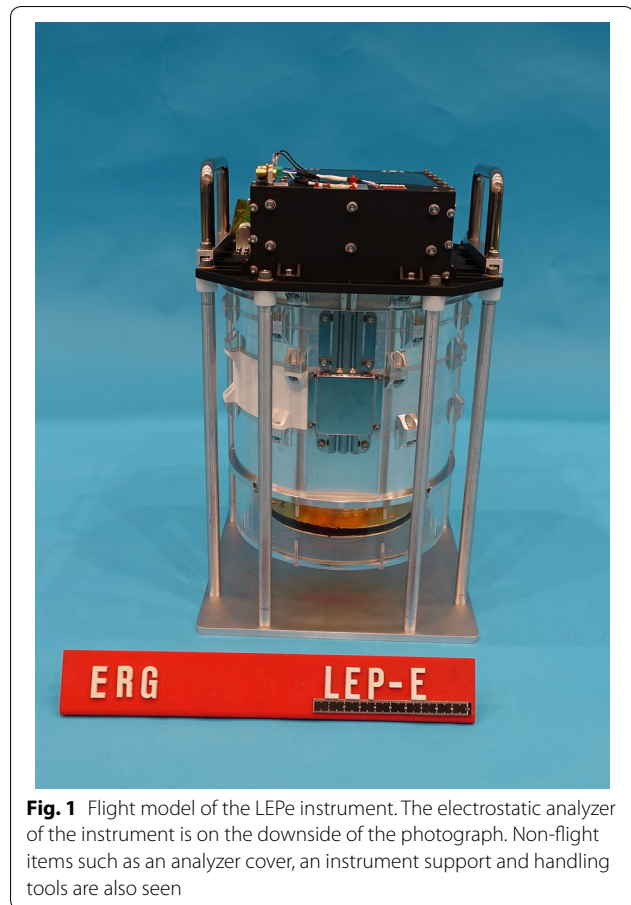


Fig. 1 Flight model of the LEPe instrument. The electrostatic analyzer of the instrument is on the downside of the photograph. Non-flight items such as an analyzer cover, an instrument support and handling tools are also seen

white paint (UPI WHITE LT48) is painted on a part of sensor housing surface opposite to the sun to enhance heat radiation into space. The thermal emissivity ϵ of this paint is estimated to be 0.8, based on measurement. The PSU housing is coated with Aeroglaze Z306 (non-conductive polyurethane coating) with high absorptivity and emissivity ($\alpha = 0.90$ and $\epsilon \leq 0.95$, according to the datasheet).

The structure inside the instrument is shown in Fig. 2. The LEPe instrument employs a toroidal tophat-type electrostatic analyzer for a good sensitivity (Carlson et al. 1983; Young et al. 1988). After the analyzer shells, a micro-channel plate (MCP) assembly holds Z-stacked MCPs with a mesh electrode and an anode board. The design and performance of the analyzer are described in the next section.

The anode board has 23 discrete anode channels, and thus, each channel has a charge-sensitive preamplifier Amptek A111E. A preamplifier is populated on a separate small-size (47.5 mm \times 32.0 mm) PCB (printed circuit board). The preamplifier PCBs are positioned radially, as shown in the figure. MCP anodes and amplifiers are connected with beryllium copper pins and sockets.

Table 1 Summary of the LEPe instrument specifications

Parameter		Unit	Remark
Dimension	180.0DIA × 204.5H	mm	Upper cylinder part
	193.0D × 131.0W × 64.0H	mm	Lower box part
Mass	5.512	Kg	
Power consumption	8.8	W	44 V, 0.20 A, incl. PSU's efficiency
Raw data production	24.6	kbyte/spin	Science data, w/o compression
G-factor			Incl. mesh transmission
	9.34×10^{-4}	cm ² sr keV/keV	Coarse ch, averaged
	2.15×10^{-4}	cm ² sr keV/keV	Fine ch, averaged
Energy range	19–19,000	eV	At 4 kV HV
Energy step	32	steps	
Energy resolution	9.2	%	FWHM
Field of views	2.98 × ~ 270	deg	
Angular resolution			EL × AZ, FWHM
	2.89 × 21.5	deg	Coarse ch, averaged
	3.05 × 4.71	deg	Fine ch, averaged

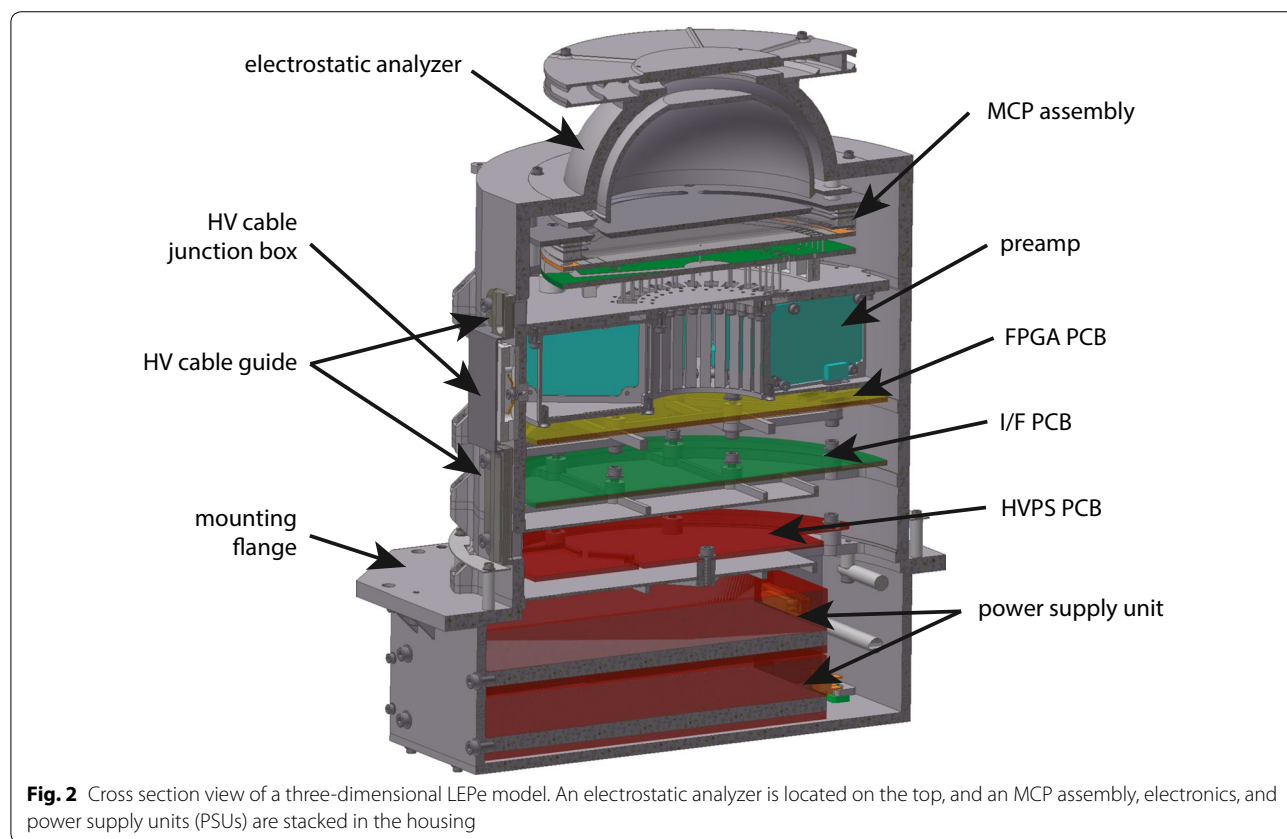


Fig. 2 Cross section view of a three-dimensional LEPe model. An electrostatic analyzer is located on the top, and an MCP assembly, electronics, and power supply units (PSUs) are stacked in the housing

Below the preamplifiers, three PCBs are stacked: FPGA (field programmable gate array) PCB, I/F (interface) PCB and HVPS (high-voltage power supply) PCB, from the top to the bottom. Each PCB is 160 mm in diameter and 2 mm in thickness. HV cables run from the HVPS to the

MCP compartment along the outside surface of the sensor housing.

PSUs in the PSU housing regulate spacecraft bus power and supply it to the circuits of the instrument. There are two PSUs supplying power to analog and digital circuits

separately. A survival heater and its connector are placed on the bottom panel of the PSU housing.

Another component of the instrument, which is not shown in the cross section view, is the central processing unit (CPU). The CPU processes LEPe data and sends it to the MDP (mission data processor). LEPe uses the CPU installed in the LEPi instrument (Asamura et al. in preparation), and CPU resources are shared with both the LEPe and LEPi instruments.

For radiation shielding, the analyzer has 6-mm-thick aluminum shield. The sensor housing and the PSU housing have 5-mm-thick and 4-mm-thick aluminum shields, respectively. We estimate that with this shielding, a total dose of the electronics is less than 100 kRad for a nominal mission lifetime of one year.

The schematic drawing of the accommodation and the FOV of the LEPe instrument are illustrated in Fig. 3. The spacecraft coordinate system (X_{sc} , Y_{sc} , Z_{sc}) is also given in the figure. The spacecraft spins with respect to the Z_{sc} axis.

As shown in the figure, the FOV is fan shaped in the $Y_{sc} - Z_{sc}$ plane. The FOV opens approximately 270 deg. To avoid artificial effects due to the MEPI instrument body, about 60 deg of the aperture toward MEPI is intentionally closed. Due to the spacecraft spin motion, the fan-shaped FOV scans the entire sky once a spin. One spin is divided into 16 spin phases (PH). During each phase, a 32-step energy sweep is done. Thus, one energy spectrum is completed every 22.5 deg along the 'longitudinal' direction. The MCP anode channels correspond to 'latitudinal' direction, perpendicular to the spin direction.

The FOV is divided into 22 directions, corresponding to MCP anode channels. There are 10 coarse channels (CH1-CH5, CH18-CH22) whose open angle is 22.5 deg, and also 12 fine channels (CH6-CH17) whose open angle is $22.5/6 = 3.75$ deg. These fine channels are located symmetrically with respect to the $X_{sc} - Y_{sc}$ plane to resolve loss cone of electron distributions. Besides the 22 coarse and fine channels, there is a background anode channel CH0. The FOV of the background channel is

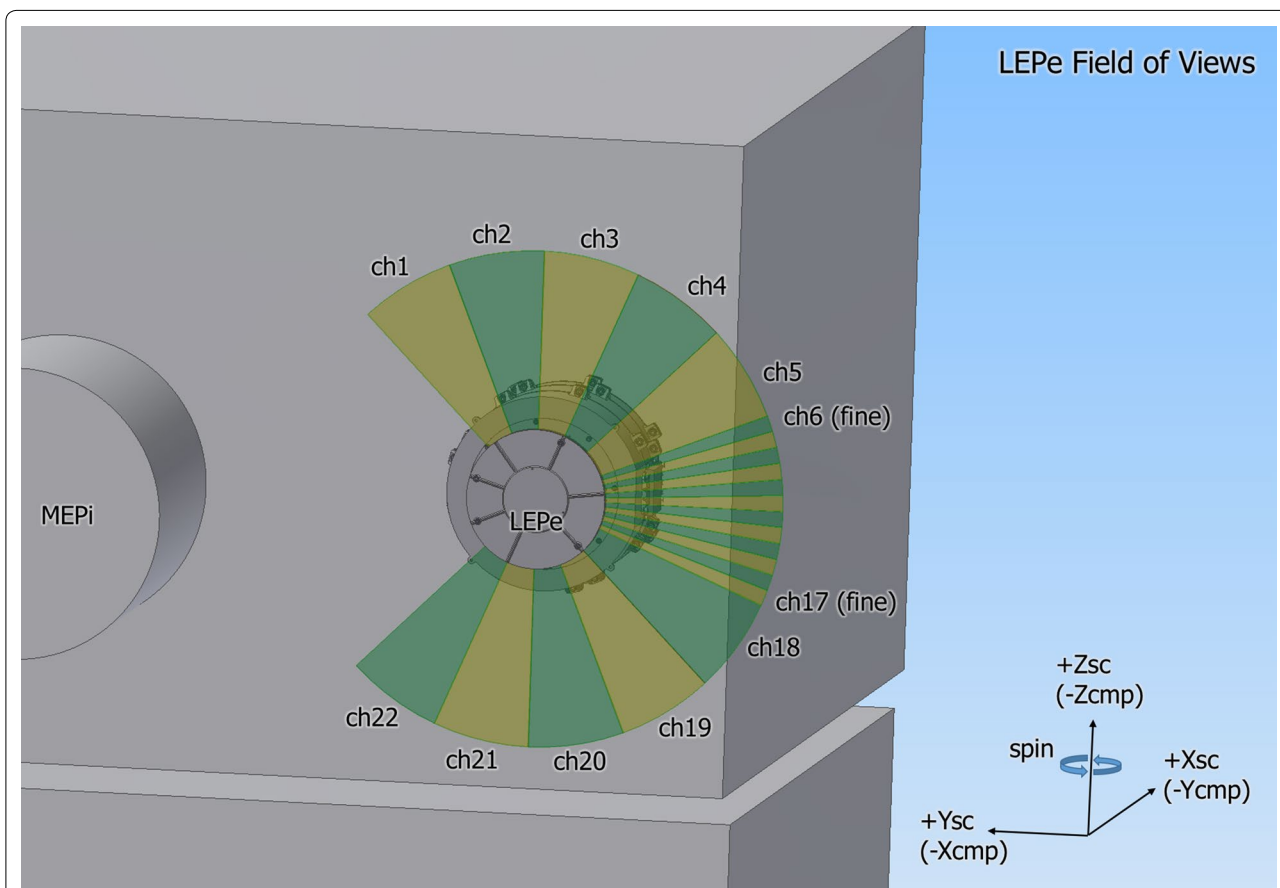


Fig. 3 Schematic drawing of the accommodation and the field of view (FOV) of the LEPe instrument. Here the suffix 'sc' stands for the spacecraft coordinate system, and 'cmp' stands for the component (instrument) coordinate system. The instrument is installed on the $-X$ panel of the spacecraft, and the fan-shaped FOV opens parallel to the panel

closed at the aperture so that this channel measures not electron counts but only background counts caused by penetrating radiation particles. The background count is subtracted to estimate electron net counts in ground data processing.

Electrostatic analyzer

Here we describe the electrostatic analyzer. As shown in Fig. 2, the LEPe instrument uses a toroidal tophat-type electrostatic analyzer.

The concept design of the analyzer is similar to the electron analyzer onboard the Reimei satellite (Asamra et al. 2003). We designed details of analyzer dimensions with requirements as follows:

- Electron energy range from ~ 12 eV to ~ 20 keV,
- Energy measurement resolution of $< 15\%$,
- Angular resolution of $< \sim 23$ deg,
- G-factor of $\sim 10^{-3}$ cm² sr keV/keV per 22.5 deg,
- Time resolution of $< \sim 8$ s.

To find the optimum design that meets the requirements, Kazama (2013) made a detailed parameter survey, considering measurement performance as well as photon suppression. The optimum design obtained was then scaled by 1.37 for the LEPe analyzer design to meet the sensitivity requirement. For the LEPe analyzer, the inner shell and outer shell radii (toroidal minor radii) are 39.5 and 43.9 mm, respectively. The bias distance (toroidal major radius) is 6.8 mm. The collimator plates are disk shaped and 64 mm in radius.

To suppress photon reflections into the detector, we use (1) fine serration machining and (2) copper sulfide (CuS) black coating. Serration is a fine saw-tooth structure (0.5 mm pitch and 0.2 mm depth) and diminishes forward reflection of photons. The serrations are machined on the inner and outer shell surfaces. CuS coating traps photons by its fine crystal shape. CuS coating is applied to the inner surfaces of the collimator plates and also to the outer and inner shells.

Electrons are detected by Z-stacked MCPs. The MCP is 114 mm in outermost diameter, 1 mm thick, and is made by Hamamatsu Photonics. The MCP assembly has an etched mesh electrode above the MCP input surface. Nominally ~ -11 V is applied to the mesh (1) to prevent stray electrons from being detected by the MCP and (2) to repel escaping secondary electrons toward the MCP for better MCP detection efficiency. The mesh's transmission factor is 83%, and this factor is included in the g-factors shown in Table 1. To the MCP input surface, $\sim +300$ V is nominally applied to enhance an electron detection efficiency of the MCP.

The MCP input surface is located 15.5 mm below the shell deflection end. This location is determined for beam electrons off the symmetric axis to focus on a single location on the MCP, so that an azimuthal angle resolution is improved. This is important to provide a high angular resolution to the fine channels.

It is noted that for this analyzer system, no coincidence or anti-coincidence techniques are employed for simplicity and robustness. Instead, we use a passive shielding method to suppress radiation counts. According to the study of the optimum thickness of shielding, the analyzer is designed to have at least 6 mm thickness of aluminum. A shield thickness and estimated background counts are discussed later in this report.

Energy angle response

To practically verify the performance of the analyzer, we tested the flight model at the particle instruments calibration facilities in ISAS. It is noted that analyzer performance tests were done by using an N₂⁺ ion beam with the analyzer voltage reversed to negative by using an external power supply.

Figure 4 shows an energy versus elevation angle response of CH18 (coarse channel). Color-coded pixels are normalized counts, and a particle-tracing calculation result is indicated by contour lines. The response shows a good agreement with the calculation result, indicating that the analyzer is well fabricated and works as expected.

The peak of the elevation angle response is seen at roughly 0 deg, and the elevation angular resolution is 2.89 deg (FWHM). This elevation angle response is designed for the analyzer not to see the spacecraft body. The energy resolution ΔK is 0.44 keV/kV, and the relative resolution $\Delta K / \langle K \rangle$ is 9.2%. The other channel data are also consistent with the calculation result.

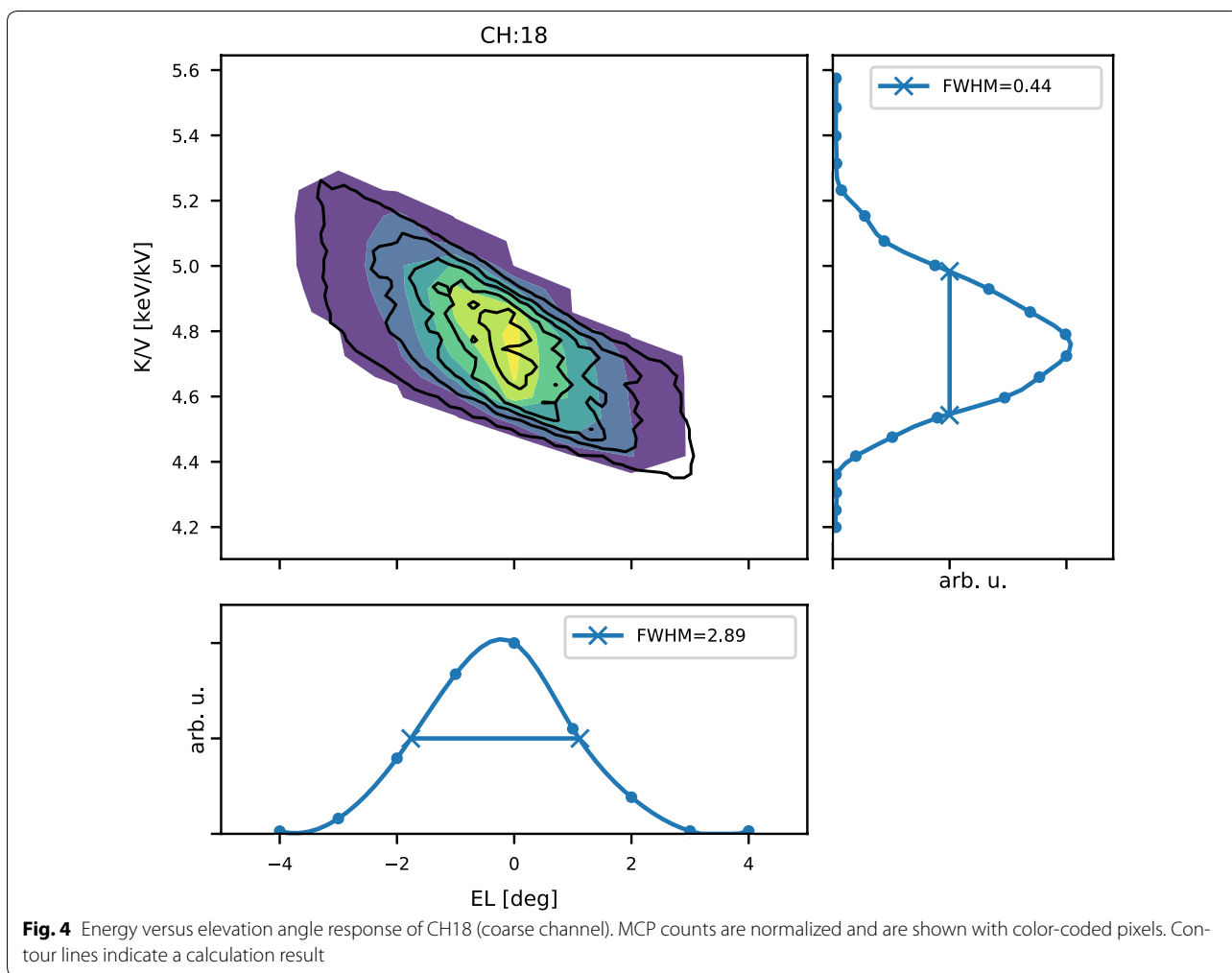
Azimuthal angular response

Azimuthal angular responses of MCP anode channels are given in Fig. 5. These data are taken with a beam fixed at EL = 0 deg. Here θ is an azimuthal angle of the analyzer to the input beam, and the origin of θ is at the boundary between CH11 and CH12.

It is seen that all coarse channels and fine channels are separated. The response drops at the CH3–CH4 and CH18–CH19 boundaries due to MCP slit supports. According to the calibration test, the average azimuth angle resolutions of coarse channels and fine channels are 21.5 deg and 4.7 deg, respectively.

Photon suppression

To estimate count rates due to sun light in flight, the analyzer's response against UV photons is measured by a



UV irradiation experiment. As a source of UV photons, a deuterium lamp is used. Figure 6 shows the response of all anode channels as a function of elevation angle. The response curves have a peak at +2.0 deg for all the channels. When EL = +2.0 deg, photons move upward, enter through the aperture, and hit the inner surface of the upper collimator. The photons then reflect downward, hit the outer shell again, and finally reach the MCP to be detected.

The peak count rates are 62–90 c/s for CH1–CH5 (coarse channel), 21–31 c/s for CH18–CH22 (coarse channel), and 6–11 c/s for CH6–CH17 (fine channels). If the spacecraft spin axis is toward the sun, solar photons always come to the analyzer in the direction parallel to the CH2/CH3-to-CH20/CH21 line (see Fig. 6).

The experiment result indicates that CH1–CH5 has higher count rates than CH18–CH22. This can be explained as backward reflection at the upper collimator. When photons hit the upper collimator, the photons reflect downward and backward toward CH1–CH5.

Considering that an anode area of a fine channel is six times smaller than that of a coarse channel, we see that CH1–CH5 show the highest counts, CH6–CH17 are second, and CH18–CH22 are third. This implies that the collimator reflects photons backward most, sideward less, and forward least.

The averaged count rate of Maxwellian electrons with a density of $1/\text{cm}^3$ and a temperature of 1 keV is ~ 8900 c/s, which is considerably larger than the maximum photon count rates of ~ 90 c/s. In addition, a sun-spin angle is kept at ~ 15 deg and thus the analyzer does not receive the photon input except during 0.26 s when the angle to the sun becomes to be 2 deg (peak elevation angle) due to the spin motion, on the assumption that the spin period is 8 s and the width of the elevation angle response is 3 deg. This is a short time period in comparison with the spin period, and also we can identify which energy steps may receive photon counts to be subtracted with spacecraft attitude information.

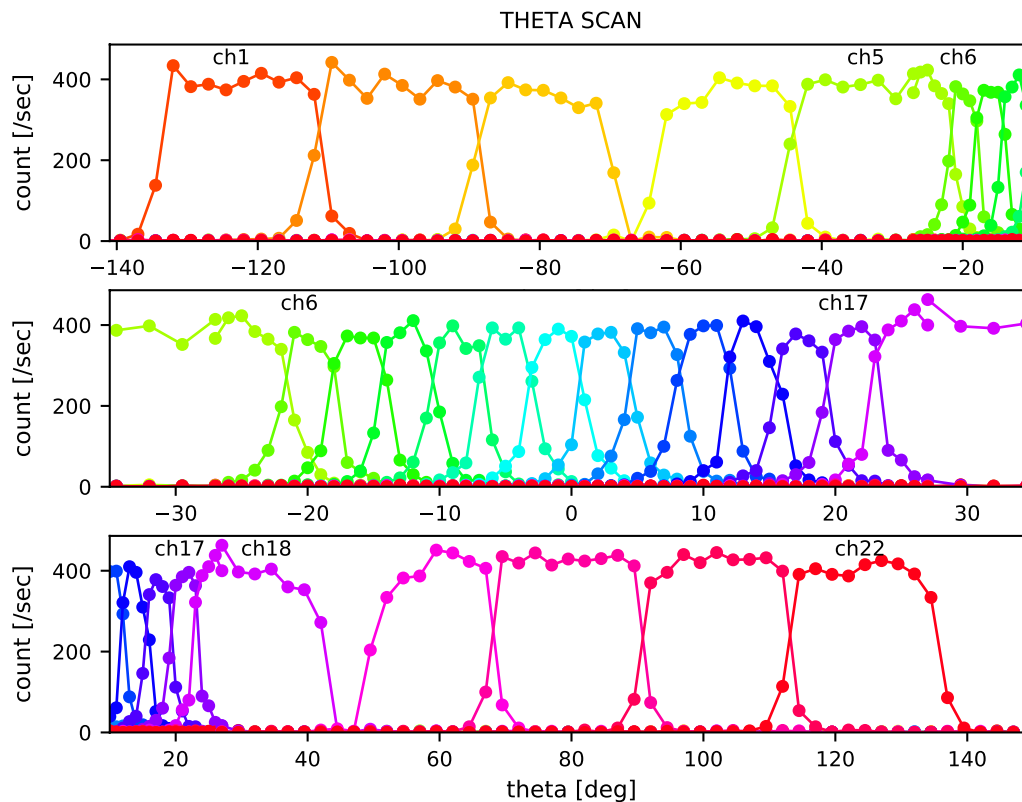


Fig. 5 Angular response of the MCP anode channels. The response is taken with a horizontal ($EL = 0$ deg) beam. The top and bottom panels are for coarse channels, and the middle panel is for fine channels. Since the background channel CH0 does not have a field of view, CH0 data are not shown

Through this experiment, analyzer's response to UV photons is compiled as a function of both elevation and azimuth angles for each channel. Hence, photon counts can be subtracted from the raw counts during data processing.

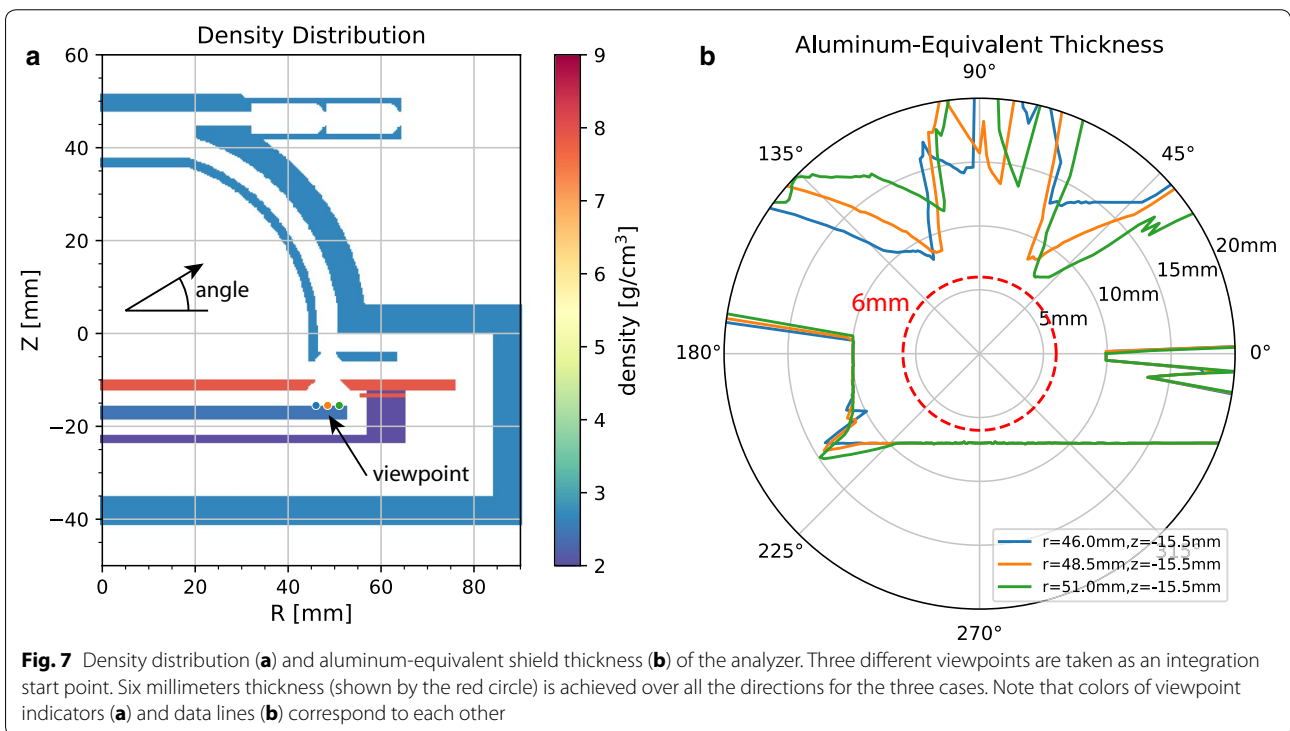
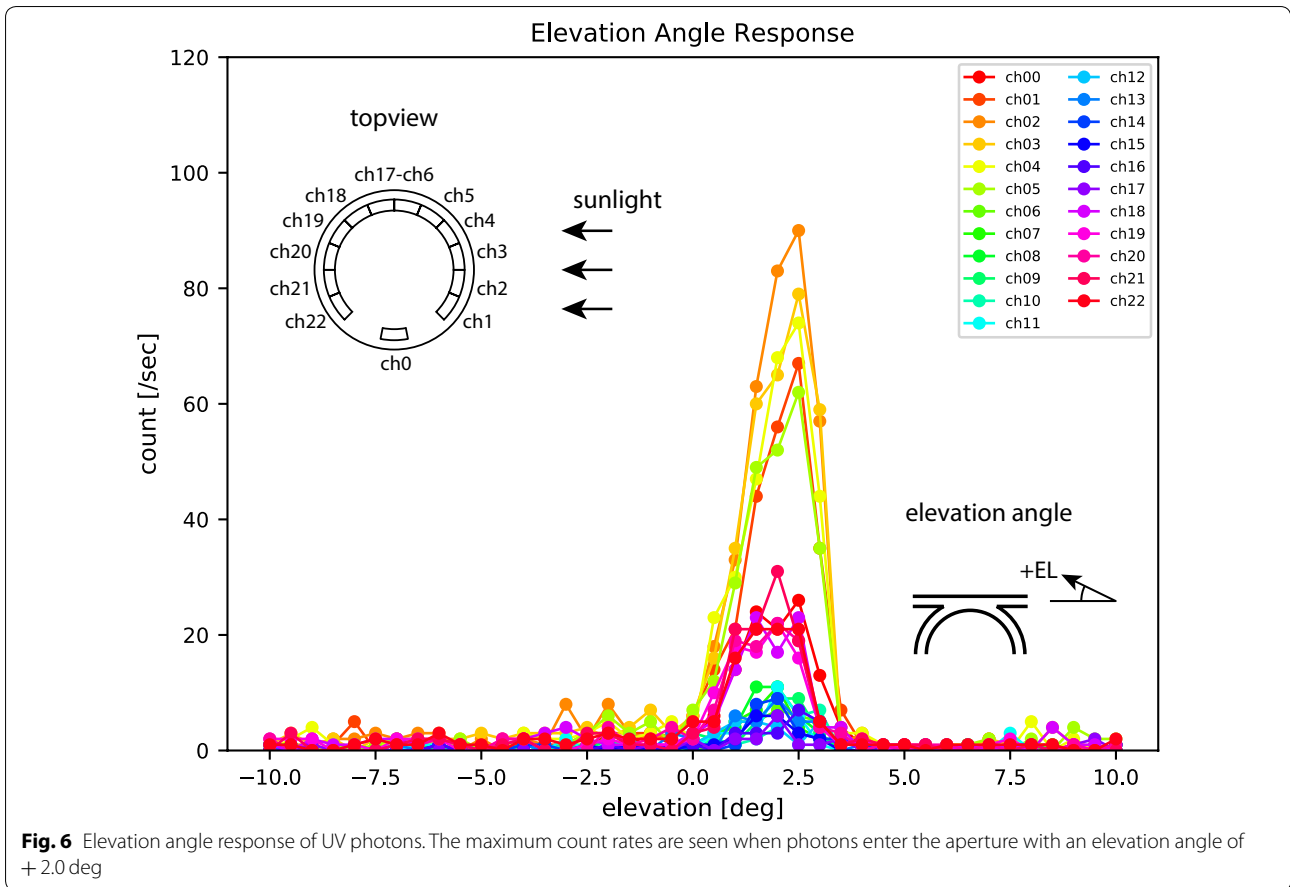
Radiation shielding

Radiation shielding is an important technical problem for low-energy electron measurement under radiation environments. As mentioned above, LEPe does not use active shielding techniques such as coincidence detection or anti-coincidence rejection, but uses a simple passive shielding method.

The analyzer has at least 6 mm thickness of aluminum shield to the MCPs to reduce radiation effects. This thickness is determined based on Geant4 simulations (For Geant4, see the web page: <http://geant4.cern.ch>). In the simulations, we virtually input radiation particles to an aluminum shield and trace tracks of the particles including effects of particle-matter interactions. Finally, fluxes of forward-scattered particles were calculated. As an input, the radiation electron models AE8 (Vette 1991) and proton model AP8 (Sawyer and Vette 1976) were used.

The Geant4 calculation indicates that output electron fluxes decrease as the thickness increases, but high-energy photons produced by electron breaking radiation show nearly constant fluxes, independent of the thickness. This is because high-energy photons such as gamma rays cannot be easily stopped. The electron flux becomes smaller than the gamma ray flux at a thickness of ~ 5 mm. Thus, a total flux does not decrease as fast as it does before 5 mm. Although a thicker shield still has a higher stopping power, the weight of the instrument also increases. Therefore, we have decided to use 6-mm-thick shields for the analyzer as a good compromise.

To verify that 6 mm thickness is ensured, a total thickness from the MCP position is calculated by integrating densities of the analyzer structures for a given direction from an MCP position. The density distribution and aluminum-equivalent thicknesses calculated are illustrated in Fig. 7. In the calculation, three viewpoints are taken: $R = 46.0, 48.5$ and 51.0 mm on the MCP input surface at $Z = -15.5$ mm (shown as circles in different colors). It is noted that all the structures below the MCP assembly are simplified and are represented as a 6-mm-thick aluminum wall on the bottom side of the analyzer.



The right panel of Fig. 7 gives the overall aluminum-equivalent thicknesses from the different viewpoints. Different viewpoint data are shown in different colors, which correspond to those of the viewpoint indicators in the left panel. We see the minimum thickness of 7.4 mm at $\theta = 54$ deg, which satisfies the requirement of 6 mm thickness.

Components of the LEPe electronics are 100-kRad radiation tolerant. The sensor housing that houses the electronics has 5 mm thickness of aluminum, which ensures a total dose less than 100 kRad for the one-year nominal mission life. Since the PSU housing is enclosed by the spacecraft panels, the housing thickness is designed to be 4 mm.

Estimated radiation counts

After the analyzer design is fixed, simulations of detailed radiation–matter interactions were made to estimate in-flight count rates due to near-earth radiation by using Geant4. The analyzer structure and its materials were modeled as shown in Fig. 7. We assumed 4π -sr AE8 and AP8 radiation fluxes as an input.

To obtain MCP counts, we need to assume detection efficiencies of MCPs for electrons, protons, and photons with radiation energies, *i.e.*, ~ 10 keV to ~ 10 MeV range. Quantum efficiency of electron multipliers such as MCPs is known to depend on particle impact energy, but this correlation is ambiguous and cannot be well determined [*e.g.*, see Fig. 2 in Bennani et al. (1973)]. Wiza (1979) summarizes absolute efficiencies in previous reports: 10–60% for 2–50 keV electrons, 4–60% for 50–200 keV ions. Bennani et al. (1973) collect experiment results of electron efficiencies, in which the efficiency ranges roughly 10–40% in energies from 10 to 100 keV. Considering that an efficiency curve decreases in a radiation energy range, we assume constant efficiency values of 10% for both electrons (positrons) and ions. For gamma ray photons, 1% of efficiency is assumed according to Wiza (1979), Tanaka et al. (2007).

Results of the simulations are summarized in Fig. 8. Estimated count rates in the figure are per coarse channel (22.5-deg wide). Counts of electrons (and few positrons), protons, and gamma ray photons are all summed into a single data point. It should be noted that we use AP8/AE8 model fluxes at the magnetic equator where the maximum radiation fluxes exist. Due to the orbit inclination, the Arase spacecraft does not always stay at the magnetic equator. Therefore, this simulation results can be overestimated compared to the reality.

The primary target region in the ERG mission corresponds to the Earth's outer belt, where a background count rate of ~ 1400 c/s can be received at each coarse channel, according to the result. In principle, background

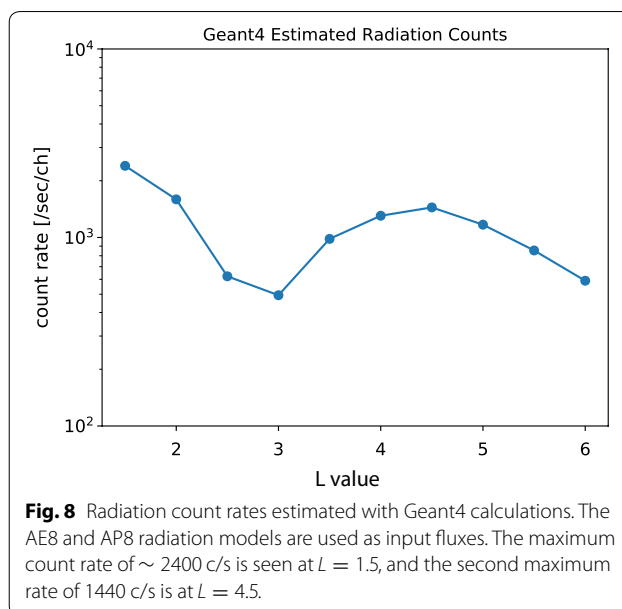


Fig. 8 Radiation count rates estimated with Geant4 calculations. The AE8 and AP8 radiation models are used as input fluxes. The maximum count rate of ~ 2400 c/s is seen at $L = 1.5$, and the second maximum rate of 1440 c/s is at $L = 4.5$.

counts will be subtracted from total counts to obtain net counts of electrons.

For a Maxwellian electron distribution with $T = 1$ keV and $n = 1$ /cc, LEPe receives the maximum electron count rate of 46,000 c/s at 2 keV. In this case, the energy range where electron counts are larger than 1400 c/s is from 140 eV to 3.8 keV. This energy range corresponds to roughly 60% of instrument energy range in a logarithmic scale. Although the background count rate of 1400 c/s is not negligible, electron count rates still exceed the background count over a wide range of energy.

Electronics

Figure 9 illustrates a block diagram of the LEPe electronics. Functions of the electronics are (1) to count MCP signals, (2) to output data to the telemetry system, (3) to receive commands, and (4) to control operations of the instrument. For these purposes, the electronics consists of 23 preamplifiers, FPGA circuit board, interface (I/F) circuit board, and HVPS board. In addition to the main electronics, the LEPe instrument also uses the CPU board installed in the LEPi instrument for further data processing and data format editing. A multitasking real-time operating system is running on the CPU, enabling CPU resources to be shared with LEPe and LEPi processes.

The MCP assembly has 23 discrete anodes, and an anode feeds the MCP's charges to an Amptek A111F charge-sensitive preamplifier. Each preamplifier has its own small PCB for better signal separation and easier testing. Besides the preamplifier PCBs, there is another PCB of the same shape, which supplies a voltage to the mesh electrode in the MCP assembly.

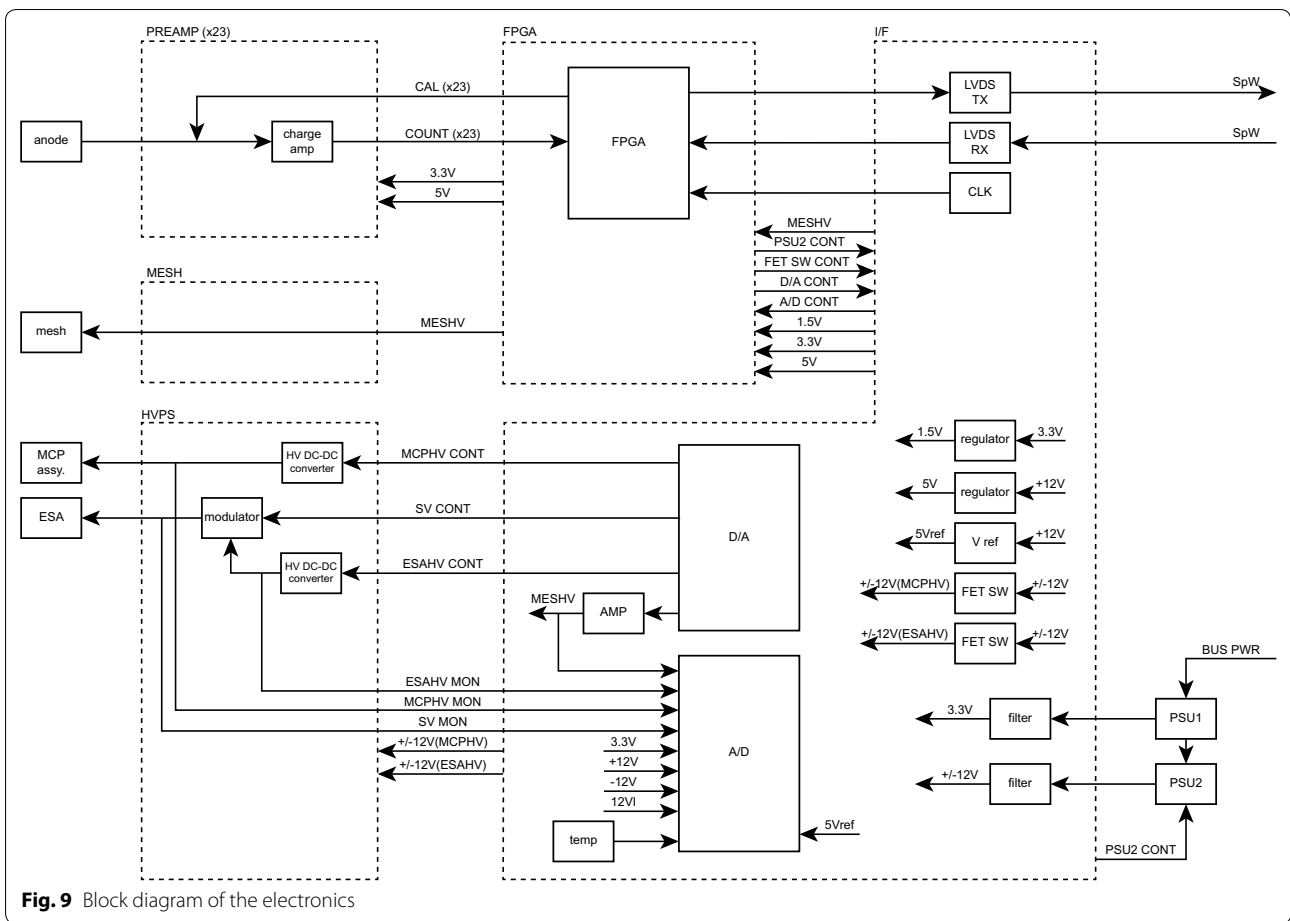


Fig. 9 Block diagram of the electronics

The preamplifier’s output goes to the FPGA PCB and is counted at counters in the FPGA. Then, the counts data are sent to the SpaceWire network through driver ICs on request from the CPU and are finally processed on the CPU and are sent to the telemetry system of the spacecraft. The FPGA also controls the LEPe instrument operations: HVPS turn on/off and output monitor/control status, sensor command decoding, HK (housekeeping) data collection, calibration pulse generation, spin synchronization, and so on.

The I/F circuit has voltage regulators, SpaceWire driver/receiver, a 12-bit DAC (digital-to-analog converter), and a 12-bit ADC (analog-to-digital converter). A temperature sensor is also placed on the I/F PCB for the reference temperature of the instrument electronics.

The HVPS board supplies two high voltages to the energy analyzer and the MCPs. Maximum voltages are 3.8 kV for the MCP and 4.1 kV for the analyzer, respectively. Both the high voltages are generated by PICO’s high-voltage DC–DC converters. For energy sweeping, the analyzer’s HVPS has two high-voltage optocouplers Amptek HV801 to modulate the output. The flight

model HVPS with the HV801 optocouplers was tested for nearly 240 h of thermal cycles, and no malfunction was identified.

Below the mounting flange, the instrument has the PSU housing, in which two PSUs are installed. The PSUs regulate a satellite bus voltage down to electronic circuit voltages. PSU1 supplies + 3.3 V for digital circuits, and PSU2 supplies + 3.3, + 12 and – 12 V for analog circuits. PSU1 feeds power to the digital circuit as soon as bus power is supplied to PSU1. Therefore, the LEPe digital circuit automatically starts up when LEPe bus power turns on.

Data reduction

In this section, we explain the data reduction method. The reduction process is a key task in data processing made on the onboard CPU, and reduction parameters are chosen based on a science target and downlink capacity.

The raw count data of the LEPe instrument C can be represented with a four-dimensional array as:

$$C = C(T; PH, K, CH),$$

where time in units of spin $T = \{T_{\text{spin}1}, T_{\text{spin}2}, \dots\}$, spin phase $\text{PH} = \{\text{PH}_0, \text{PH}_1, \dots, \text{PH}_{15}\}$, energy $K = \{K_0, K_1, \dots, K_{31}\}$, and anode channel $\text{CH} = \{\text{CH}_0, \text{CH}_1, \dots, \text{CH}_{22}\}$. Data reduction can be made along the four axes ($T, \text{PH}, K, \text{CH}$) independently.

Reduction mode

Data reduction is made by reducing a number of data along a given axis. There are two modes for data reduction, *i.e.*, ‘sum’ reduction mode and ‘skip’ reduction mode. For a data set $\{C_a, C_b, \dots, C_z\}$, a single value C results from reduction:

$$C = \begin{cases} C_a + C_b + \dots + C_z & \text{for sum,} \\ C_z & \text{for skip.} \end{cases}$$

Reduction process

Actual data reduction is as follows: First we divide values in a data set into groups and then apply reduction in ‘sum’ or ‘skip’ to each group. For example, we divide spin phase data $\text{PH} = \{\text{PH}_0, \text{PH}_1, \dots, \text{PH}_{15}\}$ into $\{\{\text{PH}_0, \text{PH}_1\}, \{\text{PH}_2, \text{PH}_3\}, \dots, \{\text{PH}_{14}, \text{PH}_{15}\}\}$, to which we apply reduction, resulting in the downsized data set $\{\text{PH}_{0,1}, \text{PH}_{2,3}, \dots, \text{PH}_{14,15}\}$.

In this process, there are two parameters: reduction mode (‘sum’ or ‘skip’) and a number of reduction data N . Because raw spin phase has 16 data, a number of reduction data points $N(\text{PH})$ can be 16, 8, 4, 2 or 1. Energy steps have 32 data points so that $N(K)$ is 32, 16, 8, 4, 2, or 1. Concerning data reduction over time, $N(T)$ must be a power of two, such as 1, 2, 4, 8, \dots .

Reduction in channel data

In contrast to the other data sets, channel data reduction has two sum modes, that is, ‘sum-A’ and ‘sum-B’, in addition to ‘skip’:

$$C = \begin{cases} C_a + C_b + \dots + C_z & \text{for sum-A,} \\ \frac{1}{N} (C_a/G_a + C_b/G_b + \dots + C_z/G_z)(G_a + G_b + \dots + G_z) & \text{for sum-B,} \\ C_z & \text{for skip,} \end{cases}$$

where G_x is a g-factor for channel x . We note that C is a floating-point number when ‘sum-B’ is selected.

A flux j is then calculated:

$$j = \begin{cases} C/(G_a + G_b + \dots + G_z) & \text{for sum-A or sum-B,} \\ C/G_z & \text{for skip.} \end{cases}$$

$N(\text{CH})$ only accepts 23, 13, 7, 5, 4, 3, 2 (including CH_0). It is emphasized that the background channel CH_0 is always independent and is never processed. If $N(\text{CH}) \leq 13$, the fine channels are first summed to two coarse channels CH_A and CH_B . Here $\text{CH}_A = \text{CH}_6 + \text{CH}_7 + \dots + \text{CH}_{11}$ and $\text{CH}_B = \text{CH}_{12} + \text{CH}_{13} + \dots + \text{CH}_{17}$. Further

reduction process ($N(\text{CH}) \leq 7$) is applied to a data set $\{\text{CH}_1, \dots, \text{CH}_5, \text{CH}_A, \text{CH}_B, \text{CH}_{18}, \dots, \text{CH}_{22}\}$.

Parameter setting

Every $N(T)$ spins, a three-dimensional count data array $C = C(\text{PH}, K, \text{CH})$ is constructed. The size of the array C is $N(\text{PH}) \cdot N(K) \cdot N(\text{CH})$. This array is then sent to the telemetry system as a packet. LEPe electron measurement has been mainly made with parameters: $N(\text{PH}) = 16$, $N(K) = 32$ and $N(\text{CH}) = 23$ (no reduction for PH , K and CH). According to the Arase observation strategy, $N(T)$ is switched to be $N(T) = 1$ (no reduction) or = 2, sum-A (sum over two spins), depending on spacecraft location.

Initial observation result

After the launch on December 20, 2016, the commissioning operation phase started in which instruments and components onboard the spacecraft were tested. On February 27, 2017, all the scientific instruments were turned on simultaneously for the first time in space.

An energy-time diagram of the observation on February 27 is shown in Fig. 10. Electron energy fluxes in the diagram are calculated by subtracting the background counts from the electron counts. It must be noted that absolute calibration of the MCP sensitivities has not yet been completed. The bottom panel shows channel-averaged raw counts per spin (shown in orange) and background counts per spin (in blue).

The LEPe instrument was turned on at $\sim 21:20$ and measured electrons until $\sim 01:00$, February 28. At 21:20, the spacecraft was at $L = 6.9$, MLAT = -21 deg and MLT = 5.4 h, and moved inward and northward.

The magnetic equator crossing happened at 00:38 with $L = 3.8$. The observation stopped at 01:00, $L = 3.2$ in the morning side (MLT = 8.3 h).

At the beginning of the measurement, the total raw count rate and the background count rate are $\sim 6 \times 10^4$ c/spin and 3×10^3 c/spin, respectively, and the background count occupies approximately 5% of the total raw count. The background count ratio to raw count is less than 10% until 00:30, and the ratio is still kept at $\sim 20\%$ at the end of the observation. In such situation, electron counts still keep a good accuracy after background count subtraction.

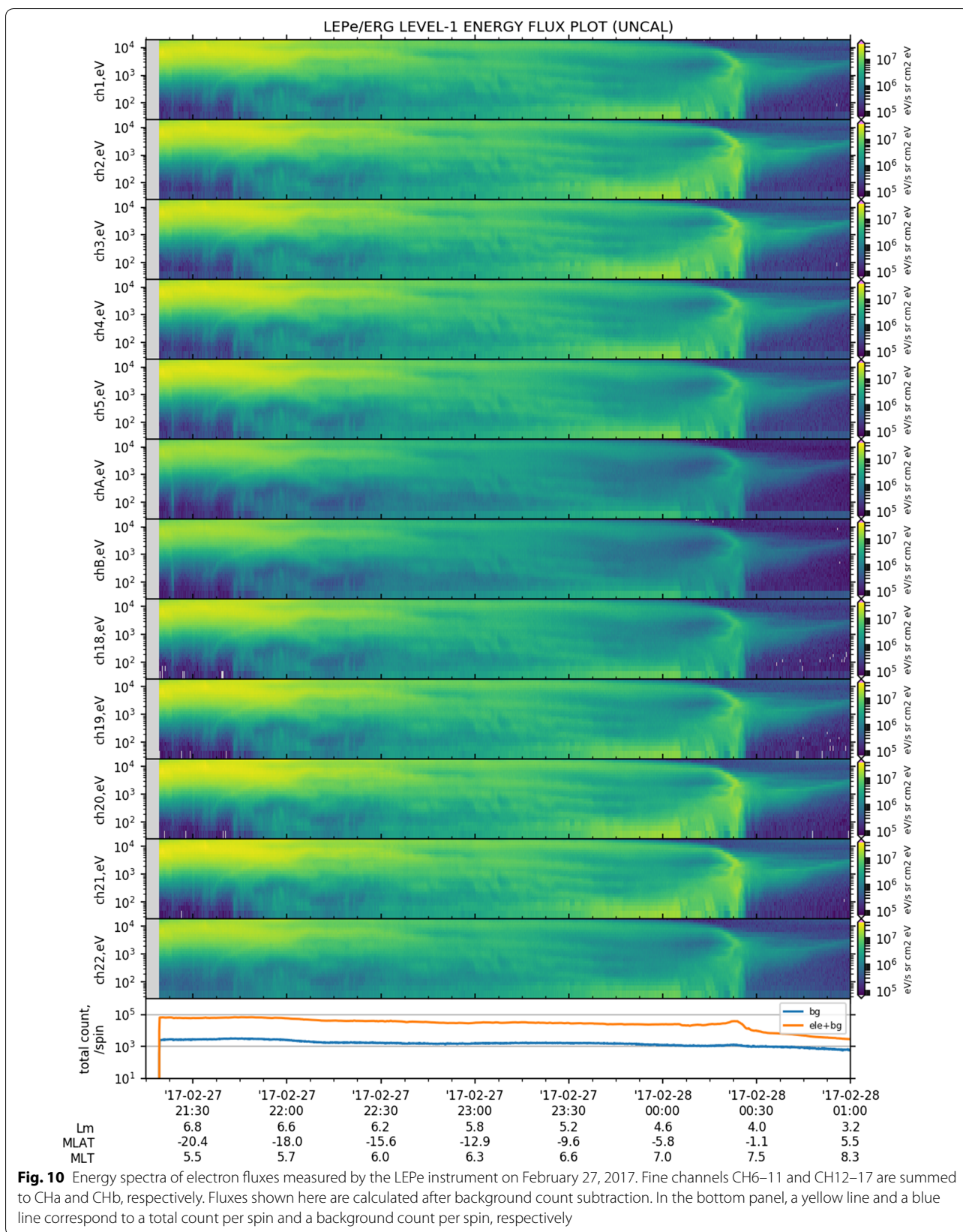


Fig. 10 Energy spectra of electron fluxes measured by the LEPe instrument on February 27, 2017. Fine channels CH6–11 and CH12–17 are summed to CHa and CHb, respectively. Fluxes shown here are calculated after background count subtraction. In the bottom panel, a yellow line and a blue line correspond to a total count per spin and a background count per spin, respectively

At the beginning of the measurement, LEPe measured high-flux electron populations with energies of several keV or higher. The fluxes of these electrons decreased in time, and as time elapsed, multiple falling energy dispersions appeared approximately after 22:00. The dispersions lasted until 00:22, February 28, at which the Arase spacecraft went into an electron-tenuous region and the fluxes suddenly dropped. The Dst index was stable at $+1 - +3$ nT before 20UT. The index then decreased down to -13 or -14 nT on 21UT. This implies that an injection occurred after 20UT, and new plasma populations were injected into the inner magnetosphere. The injected electrons were then drifting eastward and were measured by the Arase spacecraft at the morning side as energy-falling dispersions probably due to drift velocity difference.

Since March 22, 2017, the science operations phase has started and the LEPe instrument has been measuring electron environments. LEPe is kept in the nominal measurement mode all the time, but the HVPS is turned off near the perigee ($L < 1.7$) to protect the HVPS.

Since the perigee was located in the dusk side until spring in 2017, Arase focused on electron measurements related to chorus wave science. For this reason, the time resolution of the LEPe measurement was set to 8 s ($N(T) = 1$). As the perigee moved to the dawn side, Arase switched its science target to EMIC (electromagnetic ion cyclotron) waves. Since August 29, 2017, the LEPe nominal time resolution has been set to 16 s ($N(T) = 2$) to reduce electron data production.

Authors' contributions

YK is the LEPe project engineer who designed and developed the LEPe instrument, prepared the LEPe data, and wrote this manuscript. BjW developed the LEPe instrument. SyW is the LEPe project manager. PH is the LEPe instrument Principal Investigator. ST is the LEPe project scientist. TFC assisted in instrument development. CyC supported data format documentation. KA supported the LEPe development on the ISAS/JAXA side. All authors read and approved the final manuscript.

Author details

¹ Academia Sinica Institute of Astronomy and Astrophysics, No.1, Sec. 4, Roosevelt Rd, Taipei 10617, Taiwan. ² Institute of Space and Plasma Sciences, National Cheng Kung University, No.1, University Road, Tainan 70101, Taiwan. ³ Institute for Space-Earth Environmental Research (ISEE), Nagoya University, Nagoya 464-8601, Japan. ⁴ Institute of Space and Astronautical Science, Japan Aerospace Exploration Agency, 3-1-1 Yoshinodai, Chuo-ku, Sagami-hara, Kanagawa 252-5210, Japan.

Acknowledgements

We would like to thank Y. Sato and N. Takana in Meisei Electric Co. Ltd. for fabricating and testing the key electronic components of the LEPe instrument. The LEPe development is supported by the Academia Sinica, National Cheng Kung University, and also Ministry of Science and Technology of Taiwan under Contract No. MOST 105-3111-Y-001-042 and MOST 106-2111-M-001-011. Orbit information of the Arase spacecraft is provided by the ERG Science Center, Nagoya University, Japan. Dst index is provided by the World Data Center for Geomagnetism, Kyoto University.

Competing interests

The authors declare that they have no competing interests.

Availability of data and materials

LEPe measurement data will be available on the ERG Science Center (<https://ergsc.isee.nagoya-u.ac.jp/index.shtml/en>). Dst index is available at the World Data Center for Geomagnetism, Kyoto University (<http://wdc.kugi.kyoto-u.ac.jp/aedir/>).

Ethics approval and consent to participate

Not applicable.

Funding

The LEPe development is supported by the Academia Sinica, National Cheng Kung University, and also Ministry of Science and Technology of Taiwan under Contract No. MOST 105-3111-Y-001-042 and MOST 106-2111-M-001-011.

Publisher's Note

Springer Nature remains neutral with regard to jurisdictional claims in published maps and institutional affiliations.

Received: 6 September 2017 Accepted: 19 November 2017

Published online: 11 December 2017

References

- Asamra K, Tsujita D, Tanaka H, Saito Y, Mukai T, Hirahara M (2003) Auroral particle instrument onboard the index satellite. *Adv Space Res* 32:375–378
- Asamura K, Kazama Y, Yokota S, Kasahara S, Miyoshi Y. Low-energy particle experiments—ion analyzer (LEPI) onboard the ERG (Arase) satellite. *Earth Planets Space* (in preparation)
- Bennani AL, Pebay J, Nguyen B (1973) Measurement of the absolute electron detection efficiency of a channel multiplier (channeltron). *J. Phys. E Sci. Instrum.* 6:1077
- Carlson CW, Curtis DW, Paschmann G, Michael W (1983) An instrument for rapidly measuring plasma distribution functions with high resolution. *Adv. Space Res.* 2:67–70
- Kasahara S, Yokota S, Mitani T, Asamura K, Hirahara M, Shibano Y, Takashima T (2017) Medium-energy particle experiments—electron analyzer (MEP-e) for the exploration of energization and radiation in geospace (ERG) mission. *Earth Planets Space*. <https://doi.org/10.1186/s40623-017-0752-x>
- Kazama Y (2013) Designing a toroidal top-hat energy analyzer for low-energy electron measurement. In: Oyama K, Cheng CZ (eds) *An introduction to space instrumentation*. TERRAPUB, Tokyo, Japan, pp 181–192
- Miyoshi Y, Ono T, Takashima T, Asamura K, Hirahara M, Kasaba Y, Matsuoka A, Kojima H, Shiokawa K, Seki K, Fujimoto M, Nagatsuma T, Cheng CZ, Kazama Y, Kasahara S, Mitani T, Matsumoto H, Higashio N, Kumamoto A, Yagitani S, Kasahara Y, Ishisaka K, Blomberg L, Fujimoto A, Katoh Y, Ebihara Y, Omura Y, Nosé M, Hori T, Miyashita Y, Tanaka Y-M, Segawa TT (2012) The energization and radiation in geospace (ERG) project. In: Summers D, Mann IR, Baker DN, Schulz M (eds) *Dynamics of the earth's radiation belts and inner magnetosphere*. American Geophysical Union, Washington
- Miyoshi Y, Kasaba Y, Shinohara I, Takashima T, Asamura K, Matsumoto H, Higashio N, Mitani T, Kasahara S, Yokota S, Wang S, Kazama Y, Kasahara Y, Yagitani S, Matsuoka A, Kojima H, Katoh Y, Shiokawa K, Seki K, Fujimoto M, Ono T, ERG project group, (2017) Geospace exploration project: Arase (ERG). *J Phys Conf Ser* 869:012095
- Sawyer DM, Vette JI (1976) AP-8 trapped proton environment for solar maximum and solar minimum, NASA TM-X-72605
- Tanaka YT, Yoshikawa I, Yoshioka K, Terasawa T, Saito Y, Mukai T (2007) Gamma-ray detection efficiency of the microchannel plate installed as an ion detector in the low energy particle instrument onboard the GEOTAIL satellite. *Rev Sci Instrum* 78:034501
- Vette JI (1991) The AE-8 trapped electron model environment, NSSDC/WDC-A-R&S 91-24
- Wiza JL (1979) Microchannel plate detectors. *Nucl Instrum Methods* 162:587–601
- Young DT, Bame SJ, Thomsen MF, Martin RH, Burch JL, Marshall JA, Reinhard B (1988) 2π -radian field-of-view toroidal electrostatic analyzer. *Rev Sci Instrum* 59:743–751